INVESTIGATION OF HEAT TRANSFER IN A GAS FLOW IN A TUBE WITH RADIATION TAKEN INTO ACCOUNT

V. N. Vetlutskii and V. G. Sevast'yanenko

Zhurnal Prikladnoi Mekhaniki i Tekhnicheskoi Fiziki, Vol. 9, No. 5, pp. 82-88, 1968

Using the approximate hydrodynamic equations from [1-3] we calculate the nonisothermic flow of a real gas in a tube with account for radiative energy transfer for the case of a strong frequency dependence of the absorption coefficient. For a fuller clarification of the of reabsorbed emission we consider a flow of hydrogen at a pressure of 100 atm. We show that radiation makes an appreciable contribution to the heat flux on the wall at temperatures up to 9000° K for a tube of radius 0.3 cm and up to 6500° K for a tube of radius 3 cm. Similarity of the temperature profiles in different variants is observed when the temperature on the axis is below 5000° K.

Heat transfer in a laminar flow of high-temperature gas is effected by conduction and radiation. If the considered volume of gas is transparent to radiation, the consideration of the latter is relatively simple. In dense gases, however, the radiation may be reabsorbed and in this case the calculation of transfer of radiative energy in a real spectrum with a strong frequency dependence of the absorption coefficient encounters considerable difficulties. A method of calculating radiative energy transfer with allowance for reabsorption was presented in [4-7], and we used this method in this work.

If there are high temperature gradients in the gas flows it is necessary to consider the mutual effects of the velocity and temperature distributions. The solution of the complete system of Navier-Stokes equations, however, is fairly difficult even for an incompressible fluid. In [1-3] the problem of a nonisothermic flow of gas in a tube (without radiation) was solved with the aid of approximate hydrodynamic equations which are valid for high Reynolds numbers and large distances from the entrance.

NOTATION

- x, r — physical coordinates
- r_0 — tube radius
- η — logarithmic radial coordinate
- Δ — constant of logarithmic dilatation
- U, V — longitudinal and transverse velocity components
- p — pressure
- ρ — density
- T — temperature
- μ — viscosity coefficient
- $\varkappa$ — thermal conductivity
- C_p — specific heat at constant pressure
- Q — mass flow rate
- φ — integral divergence of radiative energy flux density over spectrum
- $u_{\Delta\nu}$ — integral radiative energy density over frequency interval $\Delta\nu$
- $u_{\Delta\nu}^p$ — integral equilibrium radiative energy density
- c — velocity of light
- $\langle k \rangle$ — absorption coefficient averaged over given frequency interval
- q_1 — radiative heat flux density on wall
- q_2 — conductive heat flux density on wall
- H — enthalpy
- $H^{(1)}$ — mean-mass enthalpy
- R — Reynolds number
- p — Prandtl number
- M — Mach number

Subscripts: 0 denotes values in initial section; *, values in initial section with r = 0; i, number of frequency interval; w, values on wall.

1. We consider the heat transfer in a laminar gas flow in a tube ($M \ll 1$). At high $R = \rho_* U_* r_0/\mu_*$ in the region $x \geq 0$ at a great distance from the entrance to the tube, where the parameter $\delta = V_*/U_*$ is small ($V_* = \max V$) and $\delta \sim 1/R$ by analogy with boundary-layer theory, the complete Navier-Stokes equations can be replaced with accuracy to quantities of the order of δ^2 by the approximate equations

$$\frac{\partial \rho U r}{\partial x} + \frac{\partial \rho V r}{\partial r} = 0,$$

$$\rho U \frac{\partial U}{\partial x} + \rho V \frac{\partial U}{\partial r} = -\frac{\partial p}{\partial x} + \frac{1}{r}\frac{\partial}{\partial r}\left(r\mu \frac{\partial U}{\partial r}\right),$$

$$\frac{\partial p}{\partial r} = 0, \qquad \rho U C_p \frac{\partial T}{\partial x} + \rho V C_p \frac{\partial T}{\partial r} = \frac{1}{r}\frac{\partial}{\partial r}\left(r\varkappa \frac{\partial T}{\partial r}\right) - \varphi. \tag{1.1}$$

The derivatives $\partial p/\partial r = 0$ and $\partial p/\partial x \sim \delta M^2 \gamma p_*/r_0$ and, hence, the density, specific heat, viscosity coefficient, and thermal conductivity can be regarded as functions of the temperature alone. Henceforth, instead of $\partial p/x$ we will write the ordinary derivative. For the system of equations (1.1) in the region $\Omega(x \geq 0,\ 0 \leq r \leq r_0)$ we write the boundary and initial conditions

$$\begin{gathered} \partial T/\partial r = 0,\ \partial U/\partial r = 0, \quad V = 0 \ \text{ for } \ r = 0, \\ T = T_w, \ U = 0, \ V = 0 \ \text{ for } \ r = r_0, \\ T = T^\circ(r), \ U = U^\circ(r), \ p = p^\circ \ \text{ for } \ x = 0. \end{gathered} \tag{1.2}$$

These conditions are sufficient to find the values of $V(0,r)$ and $[dp/dx]_{x=0}$ in the initial section, and the derivatives with respect to x of the longitudinal velocity component and the temperature, which enables us to make a step along the axis. For this we have to eliminate $\partial U/\partial x$ and $\partial T/\partial x$ from the first equation of (1.1) by using the second and fourth, in which $T^\circ(r)$ and $U^\circ(r)$ are substituted. Then, for $V(0,r)$ we obtain an ordinary differential equation of the first order with parameter $[dp/dx]_{x=0}$. The two boundary conditions on V enable us to determine both the function itself and the parameter.

Formulation of problem (1.1), (1.2), however, is complicated by the fact that the initial velocity and temperature profiles can be assigned arbitrarily only at the tube entrance, and Eqs. (1.1) are valid only at a large distance from the entrance. In view of this the results of this work must be regarded only as approximate engineering calculations. Since simultaneous consideration of the powerful reabsorbed radiation and the exact hydrodynamic picture is very difficult, such calculations will be of interest.

In the proposed work the initial profiles $T^\circ(r)$ and $U^\circ(r)$ are taken from calculations of a steady electric arc. In this case the complete Navier-Stokes equations are valid up to a certain distance from the section x = 0 and after this Eqs. (1.1) become valid. We assume that Eqs. (1.1) at small δ describe approximately the whole region $x > 0$, and at $x < 0$ the same equations are valid, but with the energy release term in the energy equation. Then, when x = 0 we will have a discontinuity surface of the parameters, on which the conservation conditions derived from Eqs. (1.1) written in divergent form will be satisfied. These conditions will be as follows:

$$[\rho U] = 0, \ [p + \rho U^2] = 0, \ [\rho U H] = 0.$$

Hence, on passage across the surface x = 0 the values of U, T°, and p are conserved, and only the transverse velocity component V has a discontinuity. This is a rather rough approach, but a solution of the complete Navier-Stokes equations would considerably complicate the problem. Thus, the solution of problem (1.1), (1.2) is very approximate up to a certain distance from x = 0.

The divergence of the radiative energy flux density φ was calculated from the known temperature profile on the assumption of local thermal equilibrium. The whole spectrum is divided into a series of frequency intervals, for each of which the absorption coefficient is averaged over the frequency [4–7]. For each interval the radiative transfer equation was solved in the diffusion approximation [4–8]

$$-\frac{1}{3\langle k\rangle_i r}\frac{d}{dr}\left(\frac{r}{\langle k\rangle_i}\frac{du_{\Delta\nu_i}}{dr}\right)=u^p_{\Delta\nu_i}-u_{\Delta\nu_i} \qquad (1.4)$$

with boundary conditions

$$du_{\Delta\nu_i}/dr=0 \quad \text{for } r=0,$$

$$du_{\Delta\nu_i}/dr+{}^3/_2\langle k\rangle_i u_{\Delta\nu_i}=0 \quad \text{for } r=r_0.$$

We then determined

$$\varphi=c\sum\langle k\rangle_i\,(u^p_{\Delta\nu_i}-u_{\Delta\nu_i}).$$

Here $\langle k\rangle_i$ and $u^p_{\Delta\nu_i}$ are known temperature functions [7].

Equation (1.4) is based on the assumption that radiative energy transfer along the channel axis has little effect on the divergence of the radiative energy flux. Estimates applicable to the conditions of this work showed that such an assumption gives an error of less than 10%.

In the solution of the problem we used the condition of constancy of the mass flow rate

$$2\pi\int_0^{r_0}\rho U r\,dr=Q \qquad (1.5)$$

instead of the condition that V equal zero. This relationship is obtained by term-by-term integration of the first equation in (1.1) over the radius.

The system of equations (1.1), (1.5) and the boundary conditions (1.2) allows the dilation

$$x_1=\alpha x,\ r_1=r,\ U_1=\alpha U,\ V_1=V,$$
$$T_1=T,\ (dp/dx)_1=\alpha(dp/dx),\ Q_1=\alpha Q.$$

Hence, by the following selection of dimensionless parameters

$$x'=\frac{x}{r_0}\frac{1}{R},\quad r'=\frac{r}{r_0},\quad U'=\frac{U}{U_*},\quad V'=\frac{V}{U_*}R,\ T'=\frac{T}{T_*},$$
$$\left(\frac{dp}{dx}\right)'=\frac{r_0^2}{U_*\mu_*}\left(\frac{dp}{dx}\right),\quad \rho'=\frac{\rho}{\rho_*},$$
$$\mu'=\frac{\mu}{\mu_*},\quad \varkappa'=\frac{\varkappa}{\varkappa_*},\quad C_p'=\frac{C_p}{C_{p_*}},$$
$$R=\frac{\rho_* U_* r_0}{\mu_*},\quad P=\frac{\mu_* C_{p_*}}{\varkappa_*},\quad Q'=\frac{Q}{\pi r_0^2\rho_* U_*},$$

we can eliminate the absolute velocity from the equations. This means that the obtained solution can be converted to a flow with a similar velocity profile by a simple dilatation.

2. For convenience of calculation we replace the coordinate r' in the equation by the coordinate $\eta=\ln(1+\Delta-r')$. This makes it possible, by assigning various Δ, to dilate the wall region, where the radial gradients of the unknown functions are high.

The problem was solved by the method of finite differences using iteration. The system of equations in dimensionless form was obtained by a two-layer implicit difference scheme. The second derivatives in divergent form were represented according to Marchuk's scheme [8]; the first derivatives with respect to η were represented by asymmetric differences, which ensures the validity of the pivot method [9] in the solution of difference equations. The integral in (1.5) is replaced by a trapezoidal sum.

The procedure in solving the difference equations at each step along the axis was as follows. From the known values of the parameters on the preceding step the temperature profile was determined from the difference equation obtained from the fourth equation of (1.1) by the pivot method. Then, from the simultaneous solution of the difference equations, corresponding to the second equation in (1.1) and (1.5), (dp/dx)' and the profile of the longitudinal velocity component were obtained. Finally, from the difference analog of the first equation of (1.1) the profile of the transverse velocity component was found. This process was repeated several times, as long as the difference in the parameters in two successive iterations exceeded a prescribed value. The coefficients in the equations were determined from the parameters obtained in the preceding iteration. The equation of radiative transfer (1.4) was solved in each frequency interval by means of the temperature profile from the preceding iteration. We then determined the value of φ. As a zero approximation we took the parameters from the previous step along x.

The calculations were performed on a computer. The real properties of hydrogen at a pressure of 100 atm, calculated in [7], were tabulated. The values $\langle k\rangle_i$ and $u^p_{\Delta\nu_i}$ were taken from [7], were they were calculated for eight frequency intervals. The wall temperature was taken as 300° K.

Besides the profile of T, φ, U, and V, in the cross sections of the tube we calculated the integral radiative-energy flux density q_1 over the spectrum on the wall, the conductive energy flux density q_2, and the mean-mass enthalpy $H^{(1)}$,

$$q_1=\frac{1}{r_0}\int_0^{r_0}\varphi r\,dr,\quad q_2=-\varkappa_w\left(\frac{\partial T}{\partial r}\right)_w,$$
$$H^{(1)}=\left(\int_0^{r_0}\rho U H r\,dr\right)\left(\int_0^{r_0}\rho U r\,dr\right)^{-1}$$

These quantities are connected by the energy balance equation, which is obtained by term-by-term integration of the fourth equation of system (1.1) over the radius and over the axis,

$$Q\,[H^{(1)}(0)-H^{(1)}(x)]=2\pi r_0\int_0^x(q_1+q_2)\,dx. \qquad (2.1)$$

Relationship (2.1) was used to check the accuracy of the calculation.

3. We illustrate several calculations of a hydrogen flow, the initial data of which are presented in Table 1 (here $\nu=\max[U^\circ(r)/U_*]$).

In variants 1–3, 7 the initial temperature profiles were taken from calculations for stabilized arcs of the same radius [7], and the initial velocity profiles were calculated. In variant 8 the initial profiles of variant 3 were extended along the radius. The two initial temperature profiles (stabilized arc and parabola) and the two velocity profiles (stabilized arc and jet along wall) were taken in various combinations in variants 3–6.

Figures 1–3 shows the profiles of the temperature, divergence of radiative energy flux density, and velocities for different cross sections of variant 1. In all the figures the Arabic figure denotes the number

Table 1

Вариант	R, см	Q (г/сек)	T_*, °K	ν	$T^\circ(r)$
1	0.3	1	14.700	1	$R=0.3$ см $I=500$ а
2	0.3	1	13.600	1	$R=0.3$ см $I=100$ а
3	0.3	1	12.750	1	$R=0.3$ см $I=30$ а
4	0.3	1.31	12.750	2	$R=0.3$ см $I=30$ а
5	0.3	0.87	12.750	1	Парабола
6	0.3	1.27	12.750	2	Парабола
7	3	10	8.850	1	$R=3$ см $I=300$ а
8	3	100	12.750	1	$R=0.3$ см $I=30$ а

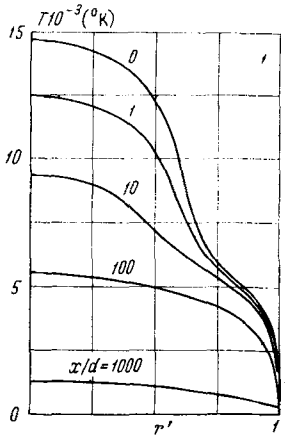

Fig. 1

of the variant according to Table 1. For the first ten calibers there is intense cooling of the gas close to the axis, mainly by radiation, which causes transverse flows towards the axis. When radiation ceases to play the main role the temperature falls over the whole radius and the transverse flows become insignificant. The profile of the longitudinal velocity component is close to a parabola in all cross sections, although the temperature varies a factor of tens. This occurred in all variants in which the profiles of stabilized arcs were taken as the initial profiles. A similar result was obtained in [10] for the region of stabilized heat transfer.

Figure 4 shows the temperature profiles for variant 3. The initial profile has a different shape, but the cooling process is similar to variant 1—the temperature at first falls only in a narrow region close to the axis. A similar situation is observed in Fig. 5 in a flow in a tube of radius 3 cm (variant 7).

The heat flux densities on the wall due to ordinary thermal conductivity and the total densities in relation to the distance along the axis are shown in Fig. 6. The circles here correspond to variant 1, the crosses to variant 2, and the triangles to variant 3. In all three cases the radiant heat flux exceeds the conductive flux. The radiation then decreases rapidly and the heat flux density due to radiation is less than 10% of the total flux for three calibers in variant 3, five calibers in variant 2, and fifteen calibers in variant 1. This instant corresponds approximately to a temperature of 9000° K on the tube axis, as is shown in Fig. 7, where the axial temperatures are plotted in relation to x/d. In addition to the symbols used in Fig. 6 the squares here correspond to variant 7. This figure shows that the axial temperature in all four variants decreases almost exponentially.

Figure 8 shows plots of the mean-mass enthalpy against the axial temperature for the same variants as in Fig. 7. The temperature profiles are not similar in the initial regions of the flow. Radiation ceases to play a role in heat transfer at about 9000° K, but the temperature profiles do not become similar until 5000° K.

Variants 3 and 8 differ only in the tube radius and, hence, comparison of them indicates the role of radiation in relation to the radius.

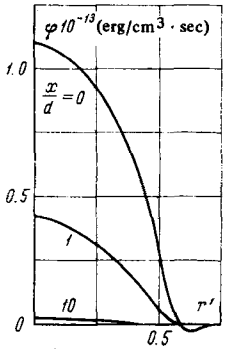

Fig. 2

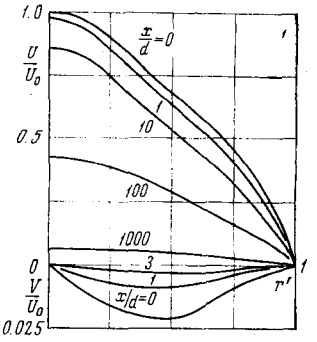

Fig. 3

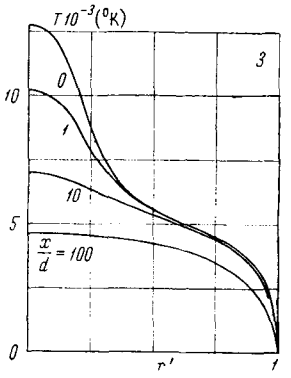

Fig. 4

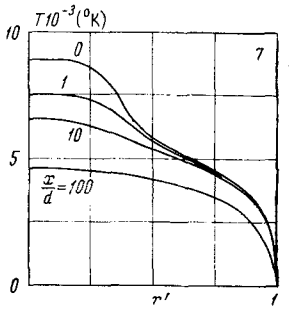

Fig. 5

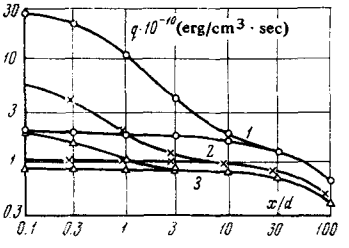

Fig. 6

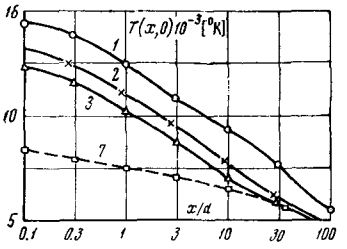

Fig. 7

Table 2

x/d	T °K	$q_1 10^{-10}$	$q_2 10^{-10}$	T °K	$q_1 10^{-10}$	$q_2 10^{-10}$
	Variant 3			Variant 4		
0	12 750	1.49	0.89	12 750	1.49	0.89
1	10 250	0.80	0.84	9 100	0.06	0.97
3	8 750	0.03	0.83	7 500	—	0.91
5	7 950	—	0.82	6 900	—	0.85
10	7 000	—	0.81	6 200	—	0.77
	Variant 5			Variant 6		
0	12 750	6,99	0.16	12 750	6.99	0.16
1	10 700	1.77	0.24	9 750	0.90	0.26
3	9 600	0.44	0.35	8 750	0.15	0.32
5	9 050	0.17	0.49	8 200	0.04	0.37
10	8 150	0.02	0.71	7 200	—	0.48

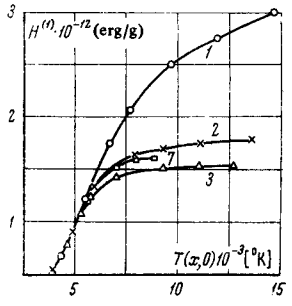

Fig. 8

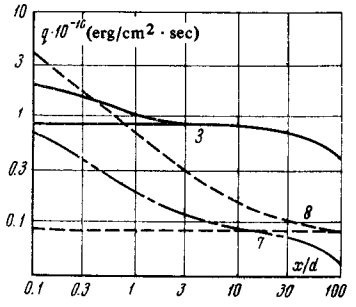

Fig. 9

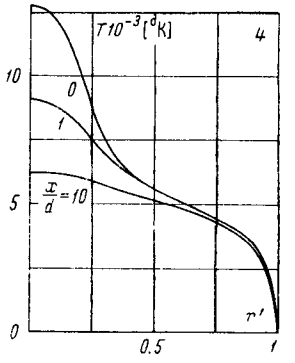

Fig. 10

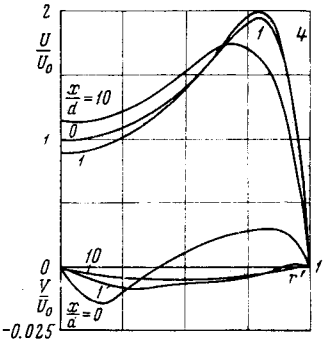

Fig. 11

Figure 9 shows the heat flux densities on the wall due to ordinary heat conduction and the total densities for variants 3, 7, and 8. The continuous lines represent variant 3, and the dashed line variant 8. In the case of a flow in a tube of radius 3 cm the density of the convective heat flux is an order less than in a tube of radius 0.3 cm, and radiation plays a greater role up to hundred calibers. Here the dot-dash line is the curve of the total heat flux density on the wall for variant 7. The heat flux density due to ordinary heat conduction merges on the graph with the corresponding curve for variant 8. Radiation plays a role up to ten calibers, which corresponds to an axial temperature of about 6500° K (Fig. 7).

In variants 3–6 the initial temperature on the axis and the initial enthalpy flow rate were made the same. This was achieved by a suitable choice of the mass flow rate. The temperature and velocity profiles obtained in variant 4 are shown in Figs. 10 and 11. A comparison of the temperature profiles in corresponding cross sections in Figs. 4 and 10 indicates that they do not differ greatly, although the corresponding velocity profiles in variants 3 and 4 differ considerably. Table 2 gives the values of the axial temperatures and the heat flux densities on the wall due to radiation and ordinary heat conduction for all four variants. The table shows that radiation disappears more rapidly in the case of a jet velocity profile and the same temperature profile. In the last two variants the temperature at the wall increases and, hence, the heat flux density due to ordinary heat conduction increases. The temperature on the axis is highest on ten calibers in variant 5. An analysis of these four variants shows that a change in the initial velocity profile from the arc type to the jet type gives a difference of not more than 15% in the axial value of the temperature on ten calibers.

The given results can, via dilation, be converted to other values of mass flow rate with the same initial temperature profile and dimensionless velocity profile.

The authors thank A. T. Onufriev for interest and assistance in the work, and also V. G. Dulov for valuable comments.

REFERENCES

1. P. M. Worsoe-Schmidt and G. Leppert, "Heat transfer and friction for laminar flow of gas in a circular tube at high heating rate," Int. J. Heat Mass Transfer, vol. 8, no. 10, p. 1281, 1965.

2. W. T. Lawrence and J. C. Chato, "Heat transfer effects on the developing laminar flow inside vertical tubes," Trans. ASME, vol. 88 C, no. 2, 1966.

3. A. P. Byrkin and I. I. Mezhirov, "Calculation of a flow of viscous gas in a channel," Izv. AN SSSR, MZhG [Fluid Dynamics], no. 6, pp. 156-158, 1967.

4. A. T. Onufriev and V. G. Sevast'yanenko, "Radiative transfer in spectral lines with self-absorption," PMTF [Journal of Applied Mechanics and Technical Physics], no. 2, 122, 1966.

5. A. T. Onufriev and V. G. Sevast'yanenko, "Calculation of radiative energy transfer in spectral lines," PMTF [Journal of Applied Mechanics and Technical Physics], no. 1, 125, 1967.

6. I. S. Voronina, V. P. Zamuraev, and V. G. Sevast'yanenko, "Calculation of radiative energy transfer in a continuous spectrum with allowance for change in absorption coefficient in relation to frequency in presence of reabsorption," PMTF [Journal of Applied Mechanics and Technical Physics], no. 1, 102, 1968.

7. A. T. Onufriev and V. G. Sevast'yanenko, "Calculation of a cylindrical electrical arc with allowance for radiative energy transfer. An arc in hydrogen at a pressure of 100 atm," PMTF [Journal of Applied Mechanics and Technical Physics], no. 2, 17, 1968.

8. G. I. Marchuk, "Methods of Calculation of Nuclear Reactors, Gosatomizdat, 1961.

9. I. M. Gel'fand and O. V. Lokutsievskii, "The pivot method for the solution of difference equations," in: S. K. Godunov and V. S. Ryaben'kii, An Introduction to the Theory of Difference Schemes [in Russian], Fizmatgiz, Moscow, 1962.

10. V. N. Popov and B. S. Petukhov, "A theoretical calculation of heat transfer and friction drag in laminar flow of steadily dissociating hydrogen in a tube," Teplofizika vysokikh temperatur, vol. 4, no. 4, p. 531, 1966.

5 March 1968 Novosibirsk